

## Computational Mechanism of Brown Seaweed (*Sargassum duplicatum*) on Non-Alcoholic Fatty Liver Disease (NAFLD)

Herin Setianingsih<sup>1\*</sup>, Peppy Nawangsasi<sup>1</sup>

1. Hang Tuah University's Faculty of Medicine, Surabaya.

### Abstract

According to estimates, 30% of Indonesia's urban population has NAFLD, with obesity being the leading risk factor. Being a maritime nation, ours has a sizable ocean region. The benefits of properly utilizing marine resources will be immense, especially when components from the marine biota are easily obtainable.

Due to its high fiber content, particularly its soluble dietary fiber, seaweed is a good source of dietary fiber. It's also critical to understand and evaluate *Sargassum*'s cholesterol-lowering mechanism. As per the research strategy plan document of Hang Tuah University, this study focuses on the technology of self-reliant medicinal raw materials. Specifically, it explores marine biota, which includes brown seaweed (*Sargassum duplicatum*), and evaluates its potential for treating Non-Alcoholic Fatty Liver Disease (NAFLD) through insilico testing.

Based on the Structure Activity Relationship (SAR) docking data, what is the role of *Sargassum* in NAFLD? Based on the Structure Activity Relationship (SAR) docking outcomes, *Sargassum duplicatum* has a role in NAFLD through Fukosterol and Fallahydroquinone.

**Experimental article (J Int Dent Med Res 2023; 16(4): 1469-1473)**

**Keywords:** *Sargassum duplicatum*, NAFLD, Fukosterol, Fallahydroquinone.

**Received date:** 26 August 2023

**Accept date:** 24 October 2023

### Introduction

People's lifestyles are becoming more sedentary, not exercising, and consuming high-fat and low-fiber foods. These changes are causing an increase in disease, with heart disease being the most common type that is becoming more common every year: Diabetes mellitus, cancer, hypertension, and coronary disease. Heart disease is the leading cause of death from heart disease in adults, with coronary heart disease (CHD) accounting for most of these deaths. Cardiovascular illnesses, including heart disease, stroke, and hypertension, are becoming more common and are now Indonesia's leading cause of mortality, particularly for those in economically active populations. The World Health Organization (WHO) said in 2017 that blood vessel disease is the leading cause of death globally. 17.7 million deaths worldwide 2015 were attributed to coronary heart disease, accounting for 31% of all

deaths. An estimated 7.4 million deaths were attributed to coronary heart disease and 6.7 million to stroke.

According to the 2021 health survey results, 3 out of 1000 Indonesians had CHD.<sup>2</sup> Because most CHD patients are in productive age, the economic burden on the nation is growing.<sup>3</sup> One of the risk factors for coronary heart disease is hypercholesterolemia. Hypercholesterolemia also raises the risk of this condition. Simple fatty liver (steatosis), fatty liver with inflammation (steatohepatitis), and fibrosis to cirrhosis are the different forms of non-alcoholic fatty liver disease (NAFLD).<sup>4</sup> It is impossible to overlook the growing public health issue of obesity, type 2 diabetes mellitus, hyperlipidemia, and non-alcoholic fatty liver disease (NAFLD). In industrialized countries, a study on obese people revealed that 60% had simple fatty liver (steatosis). Additionally, patients with type 2 diabetes mellitus were found to have 70% of them to have fatty liver, compared to around 60% in patients with dyslipidemia. Compared to people without insulin resistance, those with metabolic syndrome have a 4–11-fold increased risk of developing non-alcoholic fatty liver disease (NAFLD). According to estimates,

#### \*Corresponding author:

Herin Setianingsih,  
Hang Tuah University's Faculty of Medicine, Surabaya.  
E-mail: [herin.setianingsih@hangtuah.ac.id](mailto:herin.setianingsih@hangtuah.ac.id)

obesity is the leading risk factor for NAFLD in Indonesia's urban population, accounting for 30% of cases.<sup>5</sup> This is because obesity lowers adiponectin levels, which weakens the liver's ability to fend off fat and leads to insulin resistance. Fat liver develops due to increased triglyceride lipolysis and free fatty acid release caused by insulin resistance. Since obesity is a crucial contributing factor to the development of fatty liver, weight loss strategies involving diet control, physical activity, supplements, and medical intervention are required.<sup>6</sup> Hypercholesterolemia is also a significant factor. When using platelet-rich plasma (PRP) to treat periodontal disease.<sup>7</sup>

Extensive studies conducted on humans and animals have demonstrated the potential benefits of brown seaweed as an anti-inflammatory, antioxidant, weight-loss aid, and liver, heart, and nerve protector. Drugs that lower cholesterol levels can be used to prevent CHD and fatty liver disease (NAFLD) but are highly expensive. As a result, it is necessary to find alternatives to using natural ingredients that can reduce the risk of contracting these diseases.<sup>6</sup>

Being a maritime nation, ours has a sizable ocean region. The benefits of properly utilizing marine resources will be immense, especially when components from the marine biota are easily obtainable. Due to its high fiber content, particularly its soluble dietary fiber, seaweed is a good source of dietary fiber. Agar, carrageenan, and alginate components found in seaweed have been demonstrated in multiple studies to potentially reduce serum cholesterol.<sup>8,9</sup> Understanding and examining Sargassum's cholesterol-lowering process is also critical.

Hopefully, this research will help us determine the mechanism of Sargassum duplicatum, a natural component with antihypercholesterolemic characteristics similar to Acalypha Indica, whose mechanism is uncertain.<sup>10</sup>

As per the research strategy plan document of Hang Tuah University, this study focuses on the technology of self-reliant medicinal raw materials. Specifically, it explores marine biota, which includes brown seaweed (Sargassum duplicatum), and evaluates its potential for treating Non-Alcoholic Fatty Liver Disease (NAFLD) through insilico testing. Based on the Structure Activity Relationship (SAR) docking data, what is the role of Sargassum in NAFLD?

## Materials and methods

The 3D structures of the Sargassum bioactive compounds, namely Fukosterol and Fallahydroquinone, were downloaded from the PubChem NCBI database. The access code for the 3D structure of the Fukosterol compound is CID 5281328, while the access code for the structure of Fallahydroquinone is CID 42603805. The structure of the bioactive compound is downloaded in pdf file format and imported into the Molegro virtual docker version 5.0.0. target protein structures of MAPK1, TP53, and AKT1 were downloaded from the Protein Data Bank (PDB) database with access codes in Table 1. The 3D structures of the proteins were imported into Molegro virtual docker version 5.0.0, and the active sites of each protein used for docking were predicted<sup>11</sup> (Table 1).

No	Proteins	PDB access code	X	Y	Z	Radius	Reference
1	MAPK1	4ZZN	-12.91	14.98	42.61	9	<sup>12</sup>
2	TP53	3DCY	28.83	30.28	-8.14	11	
3	AKT1	3OCB	10.01	2.45	19.57	11	<sup>13</sup>

**Table 1.** Protein targets, protein structure access codes, and protein grids.

Fukosterol Compounds and Fallahydroquinone interact with the target protein by docking the application with Molegro virtual docker version 5.0.0<sup>14</sup>. Docking parameters with Molegro virtual docker are Score Function Moldock Score [Grid]; grid resolution 0.30; algorithm MolDock SE; Number of Runs 10, Max iterations 1500; max population size 50; pose generation energy threshold 100, tries 10 – 30; simplex evolution max steps 300; neighbor distance factor 1.00; multiple poses number of poses 5; energy threshold 0.00; cluster similar poses RMSD threshold 1. Docking results were visualized with pymol version 2.3, and the interaction was analyzed with Discovery Studio program version 21.1.1.<sup>11</sup>

## Results

Based on the three-dimensional view, the interaction of Fukosterol Compounds and Fallahydroquinone with the MAPK1 protein shows the same area. Fukosterol generates a bond energy of -298 kJ/mol to form a complex with the MAPK1 protein. Active site residues that

were bound included GLU69, ILE29, VAL37, LYS52, LEU154, and CYS164. Meanwhile, the Fallahydroquinone compound produces a bond energy of -389.8 kJ/mol, lower than the fucosterol compound. The active site residues bound by fallahydroquinone include LYS52, GLN103, ASP104, ALA33, ALA50, LEU154, ILE29, VAL37, TYR34, and MET106 (Figure 1, Table 1). Amino acid residues ILE29, VAL37, LYS52, and LEU154 were identified in the two bioactive compounds of sargassum and were inhibitory regions of the MAPK1 protein. The binding of the two bioactive compounds to MAPK1 in the inhibitory region causes MAPK1 inactivation.<sup>15</sup>

of the active fucosterol sites on the TP53 protein include ILE22, LEU100, LEU103, CYS114, PRO115, TYR92, and ILE21. All of these fucosterol residues are the active site of TP53. Fallahydroquinone also shows binding at the same site as fukosterol. Fallahydroquinone active site residues on TP53 include GLN23, ASN17, ILE21, LYS20, ALA200, ILE22, LEU100 (Figure 2). The binding energy of the fallahydroquinone – TP53 complex is -359.4 kJ/mol, lower than that of fukosterol – TP53. The binding of fukosterol and Fallahydroquinone to the active site of MDM2 on the TP53 protein causes TP53 to be free and induces transcription, and triggers cell apoptosis.<sup>16</sup>

Compound	Bond energy (kJ/mol)	Interaction	Distance	bond type	bond type
Fukosterol	-298	:10:H37 - A:GLU69:OE2	1.6945	Hydrogen Bonds	Conventional Hydrogen Bonds
		A:ILE29 - :10	5.17662	Hydrophobic	Alkyl
		A:VAL37 - :10	4.60902	Hydrophobic	Alkyl
		A:VAL37 - :10	5.46821	Hydrophobic	Alkyl
		A:VAL37 - :10	4.91006	Hydrophobic	Alkyl
		A:LYS52 - :10	4.85058	Hydrophobic	Alkyl
		A:LEU154 - :10	5.31724	Hydrophobic	Alkyl
		A:CYS164 - :10	4.75742	Hydrophobic	Alkyl
		:10:C25 - A:LEU154	4.5191	Hydrophobic	Alkyl
		:10:C29 - A:ILE29	4.46059	Hydrophobic	Alkyl
Fallahydroquinone	-389.8	A:LYS52:NZ - :10:H37	2.48167	Unfavorable	Unfavorable Donors
		A:LYS52:NZ - :10:O1	2.9923	Hydrogen Bonds	Conventional Hydrogen Bonds
		:10:H26 - A:GLN103:OE1	2.0617	Hydrogen Bonds	Conventional Hydrogen Bonds
		:10:H29 - A:GLN103:OE1	2.03167	Hydrogen Bonds	Conventional Hydrogen Bonds
		:10:H40 - A:ASP104:O	1.746	Hydrogen Bonds	Conventional Hydrogen Bonds
		A:ALA33 - :10:C25	4.13147	Hydrophobic	Alkyl
		A:ALA33 - :10:C26	4.18196	Hydrophobic	Alkyl
		A:ALA50 - :10:C27	3.54241	Hydrophobic	Alkyl
		:10 - A: LEU154	4.59103	Hydrophobic	Alkyl
		:10 - A: ILE29	5.13901	Hydrophobic	Alkyl
		:10 - A: LEU154	4.66736	Hydrophobic	Alkyl
		:10:C15 - A:ILE29	4.63554	Hydrophobic	Alkyl
		:10:C15 - A:VAL37	4.39506	Hydrophobic	Alkyl
		:10:C18 - A:ILE29	5.0435	Hydrophobic	Alkyl
		:10:C27 - A:VAL37	3.50378	Hydrophobic	Alkyl
		:10:C27 - A:LYS52	3.67914	Hydrophobic	Alkyl
		A:TYR34 - :10:C26	4.42699	Hydrophobic	Pi-Alkyl
		:10 - A: ALA50	3.25979	Hydrophobic	Pi-Alkyl
		:10 - A: MET106	5.38921	Hydrophobic	Pi-Alkyl
		:10 - A: LEU154	5.16032	Hydrophobic	Pi-Alkyl
		:10:H26 - :10:H29	1.44628	Unfavorable	Unfavorable Donors

**Table 1.** Interaction between Fucosterol and Fallahydroquinone with MAPK1 protein.

The fucosterol and fallahydroquinone compounds also show binding activity against the TP53 protein in the TP53 binding site with MDM2. The active site residues of p53 include Arg10, His11, Asn17, Lys20, Ile21, Ile22, Gln23, Arg61, Glu89, Arg90, Tyr92, Leu100, Leu103, Arg104, Cys114, Pro115, Phe117, Pro119, Leu125, His198, Gly199, Ala200, Arg203, Ser228, Ser204, Val229, Thr230, and Asn232. Fucosterol forms a complex with TP53 protein with a bond energy of -248.8 kJ/mol (Table 2). The residues

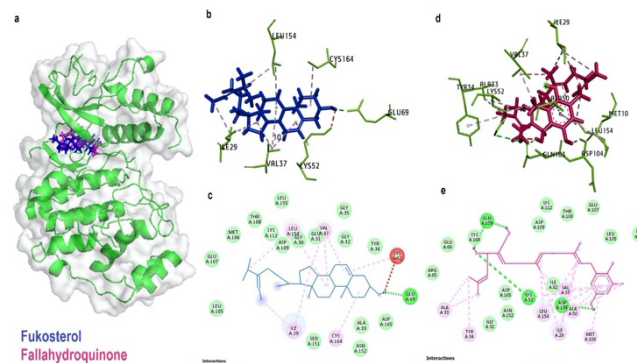


**Figure 1.** 3D and 2D structures of the Fucosterol complex and Fallahydroquinone with TP3 protein, a. superimposed ligand with protein, bc 3D and 2D structure of the fucosterol complex – MAPK1, de. 3D and 2D structures of the fallahydroquinone –MAPK1 complex.

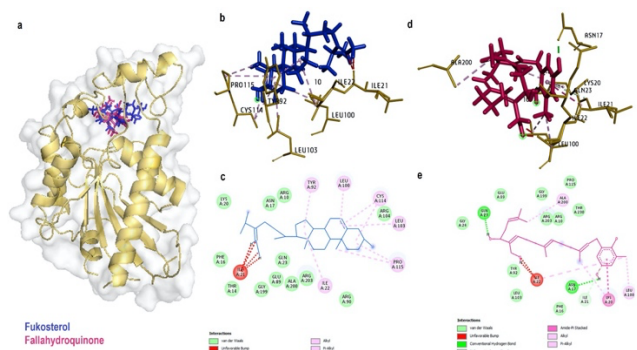


**Figure 2.** 3D and 2D structures of the Fucosterol complex and Fallahydroquinone with TP3 protein, a. superimposed ligand with protein, bc 3D and 2D structure of the fucosterol complex – TP53, de. 3D and 2D structures of the fallahydroquinone – TP53 complex.



Compound	Bond energy (kJ/mol)	Interaction	Distance	bond type	bond type
Fukosterol	-248.8	A:ILE22 - :10	4.89115	Hydrophobic	Alkyl
		A:LEU100 - :10	5.15935	Hydrophobic	Alkyl
		A:LEU103 - :10	5.41616	Hydrophobic	Alkyl
		A:CYS114 - :10	4.71089	Hydrophobic	Alkyl
		A:CYS114 - :10	5.02227	Hydrophobic	Alkyl
		A:PRO115 - :10	4.59287	Hydrophobic	Alkyl
		:10:C17 - A:PRO115	4.13457	Hydrophobic	Alkyl
		A:TYR92 - :10	4.55114	Hydrophobic	Pi-Alkyl
		A:ILE21:O - :10:C26	2.21243	Unfavorable	Unfavorable Bump
		A:ILE21:O - :10:C29	2.17157	Unfavorable	Unfavorable Bump
Fallahydroquinone	-359.4	:10:H26 - A:GLN23:O	1.75383	Hydrogen Bonds	Conventional Hydrogen Bonds
		:10:H40 A:ASN17:OD1	1.69308	Hydrogen Bonds	Conventional Hydrogen Bonds
		A:ILE21:N - :10	4.15923	Hydrogen Bonds	Pi-Donor Hydrogen Bonds
		A:LYS20:C,O;ILE21:N - :10	4.15703	Hydrophobic	Amide-Pi Stacked
		A:ALA200 - :10:C26	4.47716	Hydrophobic	Alkyl
		:10:C18 - A:LYS20	5.15498	Hydrophobic	Alkyl
		:10:C27 - A:ILE22	4.39008	Hydrophobic	Alkyl
		:10:C27 - A:LEU100	3.4388	Hydrophobic	Alkyl
		:10 - A: LYS20	4.93082	Hydrophobic	Pi-Alkyl
		A:ILE22:CD1:B - :10:O2	1.98899	Unfavorable	Unfavorable Bump
		A:ILE22:CD1:B - :10:H29	1.45983	Unfavorable	Unfavorable Bump

**Table 2.** Interaction betweenFukosterol and Fallahydroquinone with TP53 protein.

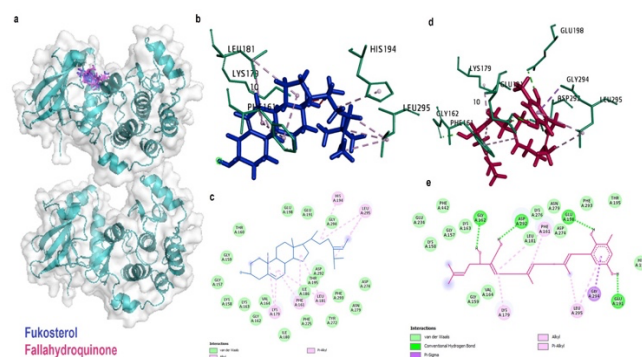


**Figure 3.** 3D and 2D structures of the Fukosterol complex and Fallahydroquinone with TP3 protein, a. superimposed ligand with protein, bc 3D and 2D structure of the fukosterol – AKT1 complex, de. 3D and 2D structures of the fallahydroquinone – AKT1 complex.

Based on the three-dimensional and two-dimensional appearance of the fukosterol – AKT1 complex, Fukosterol shows AKT1 binding at the same site as fallahydroquinone. The resulting bond energy is -305.8 kJ/mol. The active site residues of the fukosterol – AKT1 complex are LYS179, LEU181, LEU295, PHE161, and HIS194. Meanwhile, fallahydroquinone produces a lower bond energy, namely -368.8 kJ/mol. The

active sites of fallahydroquinone on AKT1 are GLY162, ASP292, GLU198, GLU191, GLY294, LYS179, LEU295, and PHE161 (Figure 3, Table 3). The active sites of fukosterol and fallahydroquinone towards AKT1 protein were identified as AKT1 inhibitory sites.<sup>15</sup>

Compound	Bond energy (kJ/mol)	Interaction	Distance	bond type	bond type
Fukosterol	-305.8	A:LYS179 - :10	4.29252	Hydrophobic	Alkyl
		A:LEU181 - :10	4.78653	Hydrophobic	Alkyl
		A:LEU181 - :10	5.34506	Hydrophobic	Alkyl
		:10 - A: LEU295	5.21605	Hydrophobic	Alkyl
		:10:C17 - A:LYS179	4.36529	Hydrophobic	Alkyl
		:10:C25 - A:LEU295	4.36625	Hydrophobic	Alkyl
		:10:C29 - A:LEU295	4.45318	Hydrophobic	Alkyl
		A:PHE161 - :10	4.51233	Hydrophobic	Pi-Alkyl
		A:PHE161 - :10	4.98755	Hydrophobic	Pi-Alkyl
		A:HIS194 - :10	4.29554	Hydrophobic	Pi-Alkyl
Fallahydroquinone	-368.8	:10:C13 - :10:H33	1.58386	Unfavorable	Unfavorable Bump
		:10:H16 - :10:H33	0.922957	Unfavorable	Unfavorable Bump
		:10:H26 A:GLY162:O	2.07033	Hydrogen Bonds	Conventional Hydrogen Bonds
		:10:H29 A:ASP292:OD2	2.25127	Hydrogen Bonds	Conventional Hydrogen Bonds
		:10:H39 A:GLU198:OE1	2.2129	Hydrogen Bonds	Conventional Hydrogen Bonds
		:10:H40 A:GLU191:OE1	1.83562	Hydrogen Bonds	Conventional Hydrogen Bonds
		A:GLY294:CA - :10	3.42786	Hydrophobic	Pi-Sigma
		A:LYS179 - :10	4.39926	Hydrophobic	Alkyl
		:10:C18 - A:LEU295	4.72164	Hydrophobic	Alkyl
		A:PHE161 - :10	5.26062	Hydrophobic	Pi-Alkyl
		A:PHE161 - :10	5.1846	Hydrophobic	Pi-Alkyl
		:10 - A: LEU295	4.96781	Hydrophobic	Pi-Alkyl

**Table 3.** Interaction between Fukosterol and Fallahydroquinone with AKT1 protein.

## Conclusions

Sargassum has a role in NAFLD through Fukosterol and Fallahydroquinone based on the results of the Structure Activity Relationship (SAR) docking.

## Acknowledgements

The Authors thank Hang Tuah University Indonesia for funding this research.

## Declaration of Interest

The authors report no conflict of interest.

## References

1. World Health Organization. *Cardiovascular Diseases*.; 2017.
2. Biro Komunikasi dan Pelayanan Masyarakat KR. Penyakit Jantung Koroner Didominasi Masyarakat Kota. <https://www.kemkes.go.id/id/home>. Published 2021. Accessed September 23, 2023.

3. Kemenkes RI. Ayo Bergerak Lawan Obesitas. *Kementrian Kesehatan Republik Indonesia*. Published online 2017:37. <http://p2ptm.kemkes.go.id>
4. Kaser S, Ebenbichler CF, Tilg H. Pharmacological and non-pharmacological treatment of non-alcoholic fatty liver disease. *Int J Clin Pract*. 2010;64(7):968-983. doi:10.1111/j.1742-1241.2009.02327.x
5. Ma'rufi R, Rosita L. Hubungan Dislipidemia Dan Kejadian Penyakit Jantung Koroner. *Jurnal kedokteran dan kesehatan Indonesia*. 2014;6(1):47-53. doi:10.20885/jkki.vol6.iss1.art7
6. Tarantino G, Citro V, Capone D. Nonalcoholic Fatty Liver Disease: A Challenge from Mechanisms to Therapy. *J Clin Med*. 2019;9(1):15. doi:10.3390/jcm9010015
7. Edith Rieuwpassa I, Minhajat R, Emelia Naomi Tetelepta F, Achmad H. *Effect of Hypercholesterolemia in Platelet Rich Plasma (PRP)*. *J Int Dent Med Res* 2019; 12(3): 980-984. <http://www.iidmr.com>
8. Amenda Saputri Mentari, Setianingsih H. Pengaruh Pemberian Ekstrak Rumpun Laut Merah (*Kappaphycus alvarezii*) terhadap Kadar LDL pada Tikus Putih (*Rattus norvegicus*) Jantan Galur Wistaryang Diberi Diet Tinggi Lemak. *Hang Tuah Medical Journal*. 2018;15(2):112-132.
9. Setianingsih H, Mutiadesi WP, Nawangsasi P. Does Chitosan Improve the Lumen of the Heart Arteries in Diabetes Mellitus? *International Journal of Innovative Technology and Exploring Engineering*. 2020;9(3S):325-327. doi:10.35940/ijitee.c1076.0193s20
10. Adisti Dwijayanti1 RWH, DGBK, SF, ARP, DS, EHP\*. Acalypha Indica and Gemfibrozil Lowering Cholesterol and Triglyceride Levels in High Fructose-Cholesterol Diet Induced Rats. *Journal of International Dental and Medical Research*. *J Int Dent Med Res* 2019; 12(2): 809-812.
11. Walter Filgueira de Azevedo Jr. *Molegro Virtual Docker for Docking. Methods in Molecular Biology*. Springer, New York; Humana; 2019.
12. Ward RA, Colclough N, Challinor M, et al. Structure-Guided Design of Highly Selective and Potent Covalent Inhibitors of ERK1/2. *J Med Chem*. 2015;58(11):4790-4801. doi:10.1021/acs.jmedchem.5b00466
13. Blake JF, Kallan NC, Xiao D, et al. Discovery of pyrrolopyrimidine inhibitors of Akt. *Bioorg Med Chem Lett*. 2010;20(19):5607-5612. doi:<https://doi.org/10.1016/j.bmcl.2010.08.053>
14. Bitencourt-Ferreira G, de Azevedo WFJ. Molegro Virtual Docker for Docking. *Methods Mol Biol*. 2019;2053:149-167. doi:10.1007/978-1-4939-9752-7\_10
15. Blake JF, Xu R, Bencsik JR, et al. Discovery and preclinical pharmacology of a selective ATP-competitive Akt inhibitor (GDC-0068) for the treatment of human tumors. *J Med Chem*. 2012;55(18):8110-8127. doi:10.1021/jm301024w
16. Ward RA, Colclough N, Challinor M, et al. Structure-Guided Design of Highly Selective and Potent Covalent Inhibitors of ERK1/2. *J Med Chem*. 2015;58(11):4790-4801. doi:10.1021/acs.jmedchem.5b00466.